Spectrochimica Acta Part A: Molecular and Biomolecular Spectroscopy 211 (2019) 221–226

Contents lists available at ScienceDirect

Spectrochimica Acta Part A: Molecular and Biomolecular Spectroscopy

journal homepage: www.elsevier.com/locate/saa

Photoluminescent properties in perylene PVD films: Influence of molecular aggregates and supramolecular arrangement

José Diego Fernandes [a], Wallance Moreira Pazin [a], Ricardo Flavio Aroca [b], Wagner Dias Macedo Junior [a], Silvio Rainho Teixeira [a], Carlos José Leopoldo Constantino [a,*]

[a] Department of Physics, School of Technology and Applied Sciences, São Paulo State University (UNESP), Presidente Prudente, SP, Brazil
[b] Professor Emeritus, University of Windsor, Windsor, On N9B 3P4, Canada

ARTICLE INFO

Article history:
Received 26 July 2018
Received in revised form 12 November 2018
Accepted 4 December 2018
Available online 4 December 2018

Keywords:
PVD thin films
Supramolecular arrangement
Aggregates
Perylene derivatives
Photoluminescent properties

ABSTRACT

Organic thin films are at the forefront of basic studies and applications in the field of physics, chemistry, biochemistry and materials science. For example, the intrinsic supramolecular arrangement, or simply the formation of aggregates may alter the optical and electrical properties, which would impact the potential applications of the material. Here, an attempt is made to correlate the molecular structures of two perylene derivatives, bis butylimido perylene (BuPTCD) and bis phenethylimido perylene (PhPTCD), with their film formation, in particular, the supramolecular arrangement and the photoluminescent properties. Emission spectra show that the PhPTCD has a radiative efficiency (RE) higher than that for BuPTCD when both are in solutions (monomers). Complementary, regarding PVD films, UV–Vis absorption measurements reveal that PhPTCD forms, predominantly, J aggregates, which are responsible for perylene derivative emission. However, BuPTCD PVD films are found to provide higher RE than PhPTCD PVD film. This apparent controversy could be explained considering other features such as crystallinity and molecular organization. The PVD film of BuPTCD is crystalline while PhPTCD PVD film is amorphous; BuPTCD has an edge-on while PhPTCD has a face-on molecular organization in PVD films.

1. Introduction

Perylene derivatives have attracted attention mainly due to their optical and electrical properties, chemical and thermal stability, controlled modifications of their molecular structure and, in addition, a high fluorescence quantum yield of nearly unity [1–3]. These features enable perylene derivative films to be used in a wide range of applications, such as light emitting diodes [4], solid state laser [5], color filter of liquid crystal displays [6], molecular probes [7], bioimaging [8], transistors [9], solar cells [10], and sensors, as for detection of dopamine [11], pesticides, and metal ions (Cu^{2+} [12] and Hg^{2+} [13]).

Several techniques have been applied to the formation of thin films, for instance Langmuir [14], Langmuir-Schaefer (LS) [14], Langmuir-Blodgett (LB) [15], spin-coating [16] and physical vapor deposition (PVD) [17]. However, among them, the latter became one of the most common technologies for deposition of small organic molecules, mainly because of the high degree of purity and good control of film thickness [18,19]. The supramolecular arrangement of perylene derivatives when forming thin films, besides their molecular aggregates, is a key factor on the optical and electrical properties of these thin films.

Supramolecular arrangement in thin films is determined by thickness, molecular aggregation and organization, and crystallinity, which may be correlated with the chemical structure of the molecule [20,21]. For instance, it has been shown that by changing the side groups attached to the perylene chromophore, different molecular organization and crystallinity can be achieved [22–25]. Furthermore, supramolecular arrangement studies regarding perylene derivative thin films have suggested the presence of H and J aggregates in the thin films, even though perylene derivatives tend to form H aggregates, preferentially [21,26–29]. This feature is also strongly dependent on the molecular structure of the perylene, mainly because it may hinder the formation of H aggregates, then favoring the formation of J aggregates [30]. This fact is important because the latter, differently of H aggregates, have fluorescent properties, being suitable for application in photovoltaic and optical devices [31].

Perylene derivatives might be synthesized in a controlled fashion, leading to particular molecular structures. For instance, the bis (butylimido) perylene (BuPTCD) has two alkyl side chains with four carbons each one, while bis(phenethylimido) perylene (PhPTCD) has two alkyl side chains with two carbons and linked to a benzene ring (Fig. 1), with the chromophore being the same for both derivatives.

* Corresponding author at: Rua Roberto Simonsen, 305, 19060-900 Presidente Prudente, Brazil.
E-mail address: carlos.constantino@unesp.br (C.J.L. Constantino).

https://doi.org/10.1016/j.saa.2018.12.009
1386-1425/

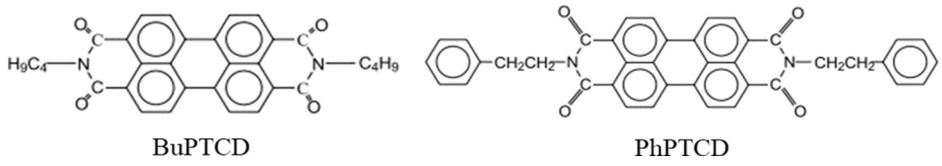

Fig. 1. Molecular structures for BuPTCD and PhPTCD.

Previous works have shown that PVD films obtained for both BuPTCD and PhPTCD perylene derivatives presented distinct supramolecular arrangements (molecular organization and crystallinity) due to their distinct molecular structures (side chains) [32,33]. However, information about the influence of such supramolecular arrangement in the spectroscopic properties of the PVD films is particularly important. The present study focuses on the correlation between supramolecular arrangement and optical properties (absorption/emission) of BuPTCD and PhPTCD in PVD thin films. In this context, not only molecular aggregation but also molecular organization and crystallinity were considered as parameters that determine the supramolecular arrangement of these PVD thin films. The use of two PTCD derivatives is to take into account also the radiative efficiency, which is as a molecular property (rather than a PVD film property).

2. Materials and Methods

The purified samples of BuPTCD (MM = 502.56 g/mol) and PhPTCD (MM = 602.15 g/mol) were provided by Dr. J. Duff from the Xerox Resource Centre of Canada. BuPTCD and PhPTCD solutions were prepared with 10% trifluoroacetic acid (TFA) in dichloromethane since the dye is insoluble in organic solvents (10^{-6} mol/L). PVD films of BuPTCD and PhPTCD were grown using the vacuum thermal evaporation technique in a Boc Edwards machine, model Auto 306, under 10^{-6} Torr, as described in [32,33]. Basically, the method consists of placing the perylene derivative powder in a Ta boat where an electric current is applied to promote the evaporation of the material. The electrical current was adjusted slowly up to 1.4 A to BuPTCD and 1.8 A to PhPTCD, leading to an evaporation rate between 0.1 and 0.4 nm/s, monitored in-situ by a quartz crystal microbalance. The PVD films were deposited in five evaporation steps onto quartz plates kept at room temperature (22 °C) up to 100 nm (mass thickness). For each step, 5.0 mg were placed into the Ta boat to be evaporated. This approach ensures a controlled growth of both BuPTCD and PhPTCD PVD films in terms of amount of material/nm deposited, as previous investigated in [32,33].

The UV–Vis absorption spectra of the PVD films of BuPTCD and PhPTCD were obtained using a Varian spectrophotometer, model Cary 50, from 200 to 800 nm. The emission spectra of the PVD films were recorded using a Renishaw micro-Raman spectrograph, model in-Via, equipped with a Leica microscope, laser line at 514.5 nm, 1800 lines/mm grating, time exposition of 10 s with a 50× objective lens, and CCD detector. This arrangement of laser, lens, and optical pathway leads to a spatial resolution around 1 μm (spot diameter of the focused laser beam). The confocal fluorescence images of the PVD film surfaces were obtained with a Nikon C2/C2si Eclipse microscope, using a 40× air objective, NA 0.9, using laser line at 561 nm and emission filter of 570–1000 nm. The crystallinity of the PVD films was investigated via X-ray diffraction carried out in a Shimadzu diffractometer, model XRD6000, with Cu-κα1 (λ = 1.5406 Å) and Cu-κα2 (λ = 1.5444 Å) radiation, 40 kV, 30 mA. The scan was performed at intervals of 2θ angles from 3.0° to 70°, using divergence and reception slits of 1°, with a step of 0.02°, and a scan rate of 2°/min. Complementary, the molecular structures of BuPTCD and PhPTCD were optimized via DFT calculation using the Lee-Yang-Parr correlation functional (B3LYP) and 6-311G (d, p) level of theory for the ground state with C1 symmetry.

3. Results and Discussion

3.1. UV–Vis Absorption Spectra

The UV–Vis absorption for perylene derivatives usually consists of electronic transition bands involving different vibrational levels

Table 1
Wavelength values for the two most intensity bands in both BuPTCD and PhPTCD solutions, as well as their blue and red shift wavelengths in their respective PVD films. Δλ is the difference between the wavelength values found in solution and in films for both BuPTCD and PhPTCD.

Perylene derivative	Solution 10^{-6} mol/L (λ nm)		PVD film (λ nm)		Blue-shift (Δλ nm)	Red-shift (Δλ nm)
BuPTCD	486	523	463	573	23	50
PhPTCD	486	523	463	612	23	89

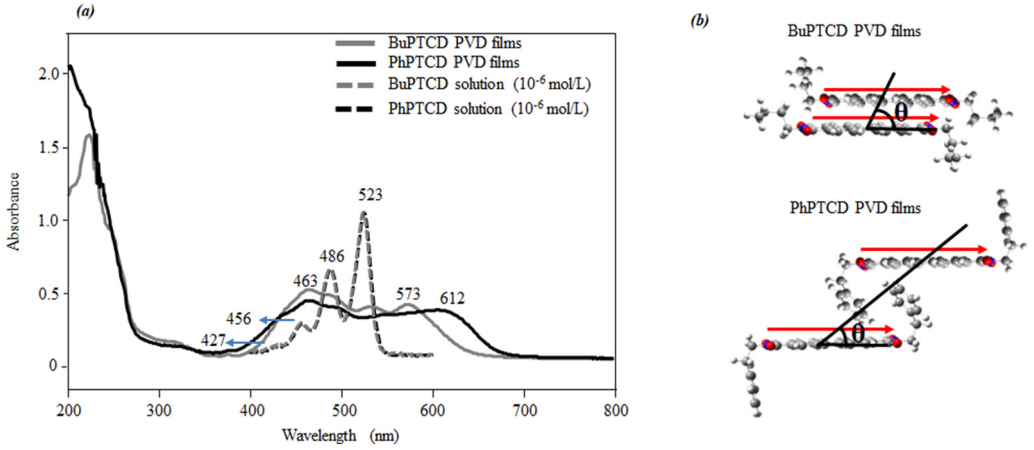

Fig. 2. (a) UV–Vis absorption spectra for BuPTCD and PhPTCD in PVD films on quartz plates (100 nm mass thickness) and in dichloro methane/TFA (90:10 v/v) 10^{-6} mol/L solution, at 23 °C. (b) Representation of the BuPTCD and PhPTCD with their respective transition dipoles and their possible "slip angle".

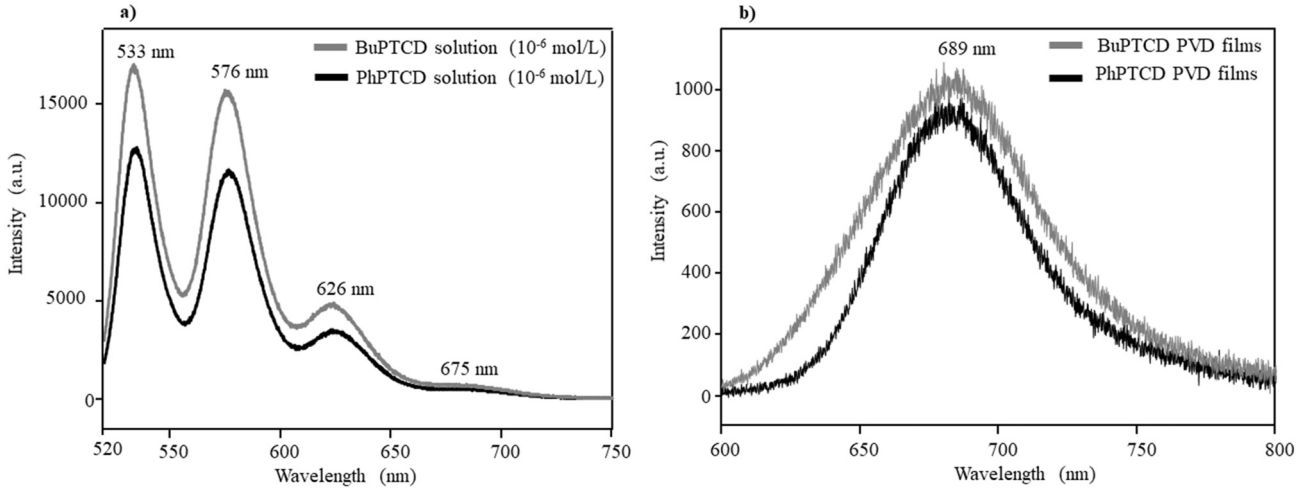

Fig. 3. Emission spectra obtained with excitation at 514.5 nm for BuPTCD and PhPTCD in: (a) dichloro methane/TFA solution (90:10 v/v), at 10^{-6} mol/L, and (b) 100 nm mass thickness PVD films on quartz plates (23 °C).

[34,35]. Fig. 2a shows the UV–Vis absorption spectra for both BuPTCD and PhPTCD in PVD films and in dichloro methane/TFA solution (90:10 v/v) at 10^{-6} mol/L.

The electronic absorption spectra of BuPTCD and PhPTCD in solution, present four main bands with maxima at 523, 486, 456, and 427 nm, which correspond to the π-π* transitions from electronic ground state (S_0) to different vibrational levels (0-0, 0-1, 0-2, 0-3) of the first electronic excited state (S_1) [36–39]. The similarity of the spectra for both BuPTCD and PhPTCD in solution indicates suggests that their lateral groups do not affect their absorption bands. However, for both BuPTCD and PhPTCD PVD films with 100 nm mass thickness, a shift (split) in the absorption bands is observed towards higher and lower wavelengths when compared to their respective solution spectra (Fig. 2a). Such effect might be consequence of molecular aggregates in the PVD films, where the red-shift refers to a head-to-tail arrangement (J-aggregates) and the blue-shift to a parallel arrangement (H-aggregates), according to point-dipole Kasha model [40].

Regarding the estimation of H- and J-aggregates, it is clear (qualitatively) in Fig. 2 that the broadening of the UV–Vis spectra for both PVD films is quite similar considering the blue-shift (H-aggregates). However, it is also clear that the red-shift (J-aggregates) is greater for PhPTCD PVD film. In addition to this qualitative description, an estimation of H- and J-aggregates could be established considering the wavelength of the two most intense bands for both BuPTCD and PhPTCD

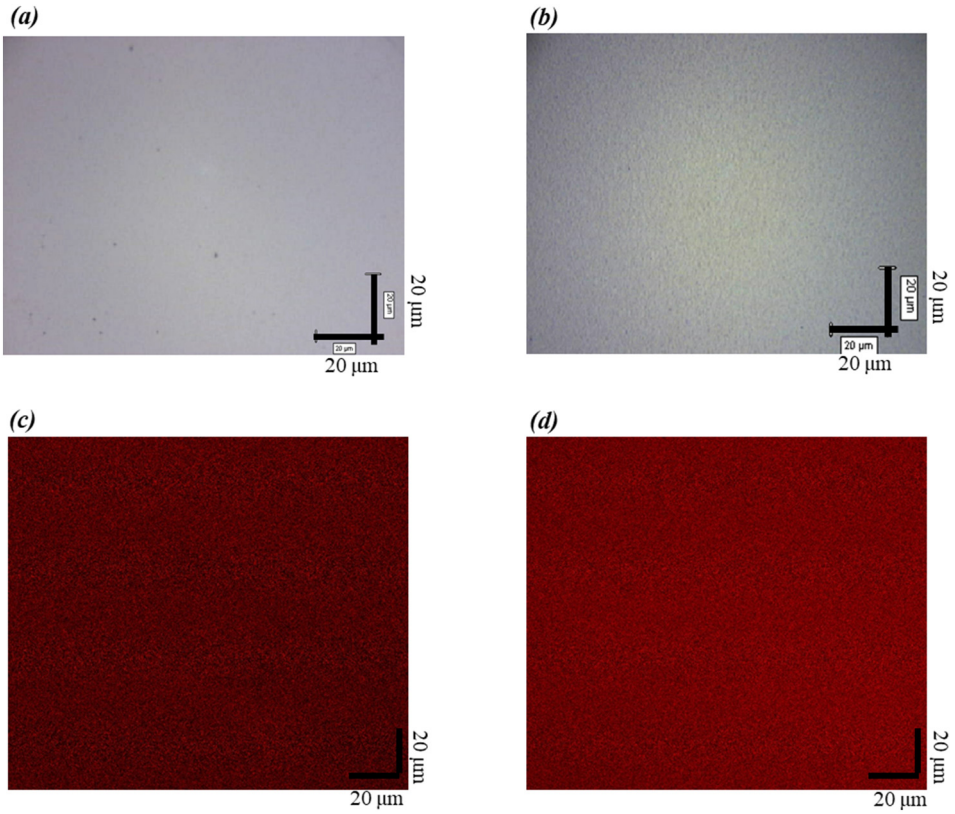

Fig. 4. 100 nm BuPTCD and PhPTCD PVD films deposited on quartz substrate: optical microscopy images for (a) BuPTCD and (b) PhPTCD; confocal fluorescence images for (c) BuPTCD and (d) PhPTCD.

Table 2
Intensity of the emission band, absorbance at 514 nm and radiative efficiency (RE) for BuPTCD and PhPTCD PVD films (100 nm mass thickness) and their solutions (10^{-6} mol/L).

Perylene derivative	Intensity (fluorescence – u.a.)		Absorbance (514 nm)		Efficiency (F / A_{514})	
	PVD	Solution (10^{-6} mol/L)	PVD	Solution (10^{-6} mol/L)	PVD	Solution (10^{-6} mol/L)
BuPTCD	8.14×10^4	1.04×10^6	0.382	0.079	2.13×10^5	1.3×10^7
PhPTCD	6.28×10^4	7.77×10^5	0.333	0.048	1.88×10^5	1.6×10^7

solutions, and the blue and red shift for PVD films. Table 1 shows the wavelength values for the peaks with maxima at 486 and 523 nm and the respective shifted values for the PVD films: basically, 463 nm (blue-shift for both BuPTCD and PhPTCD) with a wavelength difference ($\Delta\lambda$) of 23 nm; 573 nm and 612 nm (red-shift for BuPTCD and PhPTCD, respectively) with $\Delta\lambda = 50$ and 89, respectively. This estimation suggests that, besides both J- and H-aggregates are present in both BuPTCD and PhPTCD films, there is a predominance of J-aggregates (higher $\Delta\lambda$), being even greater for PhPTCD. This may be related to the presence of benzene rings in the PhPTCD side chains, which could provide an intermolecular longitudinal distance greater than that for BuPTCD [31] (Fig. 2b – structure optimized by theoretical calculations). Thus, smaller molecular slippage angle ($0 \le \theta < 57.4$) results in the formation of J aggregates while greater slippage angle ($90 \ge \theta > 57.4$) leads to H aggregates according to Kasha's exciton model [41] (the interval of θ can be changed for other dye molecules [41,42]).

3.2. Emission Spectra

Fig. 3a shows that the excitation at 514.5 nm results in emission spectra for both BuPTCD and PhPTCD solutions with four main bands with maxima at 533, 576, 626, and 675 nm, assigned to electronic transitions from the first electronic excited state (S1) to different vibrational levels at electronic ground state (S0). Such spectra are characteristic of monomeric perylene derivatives (Fig. 3a) [23]. Differently, Fig. 3b shows that at the same wavelength excitation, both BuPTCD and PhPTCD PVD films resulted in a broad emission band with maximum at 689 nm, which is assigned to excimer emission (fluorescence) [43], with absence vibrational structure.

It is important to mention that emission spectra were collected for different regions of BuPTCD and PhPTCD PVD films, and their profile and intensity were the same as shown in Fig. 3b, characteristic of a uniform distribution of the molecular aggregates over the films (Fig. 4).

The radiative efficiency (RE) of BuPTCD and PhPTCD PVD films and solutions was investigated by the ratio between the intensity (F) of the emission band (integrated area) from Fig. 3 and the value (A_{514}) of the absorbance at 514 nm (excitation wavelength) from Fig. 2a: $RE = F / A_{514}$. As shown in Table 2, the RE is 12% higher for BuPTCD compared to PhPTCD PVD film. According to UV–Vis absorption spectra in Fig. 2 (and Table 1), PhPTCD PVD film presents larger amount of J-aggregates. Therefore, because, J-aggregates are directly related to fluorescence intensity in emission processes, one would expected a higher RE for PhPTCD PVD film [30,31,44], leading to a contradictory result. Besides, by verifying the emission properties for both BuPTCD and PhPTCD as monomers (solution), it is found that the RE of PhPTCD is 19% higher compared to BuPTCD when in solution. This means that, even presenting lower amount of J-aggregates (PVD films) and lower RE (monomer), BuPTCD in PVD film presents higher RE than PhPTCD in PVD film. Therefore, other particular features of the PVD films, beyond H- and J-molecular aggregation, must be taken into account to explain the apparent contradiction found for BuPTCD PVD films (higher RE than PhPTCD forming PVD film).

3.3. X-ray Diffraction

According to Dong et al. [45], the fluorescence of 1,2-diphenyl-3,4-bis(diphenylmethylene)-1-cyclobutene increases with aggregation and intensities when such aggregates present a crystalline phase. Li et al. and Hsiao et al. also correlate the formation of molecular crystals to fluorescence increase [46,47]. The relationship between crystallinity and fluorescence improvement is explained due to the lack of intermolecular cavities as found for amorphous material, which contributes to the free molecular rotation, directly related to the non-radiative processes [47]. Therefore, the crystallinity for both BuPTCD and PhPTCD PVD films was investigated through X-ray diffraction, which results are shown in Fig. 5. Differently of PhPTCD, BuPTCD PVD film presents only a high intensity and well-defined (020) diffraction peak, characteristic of oriented crystalline material. So, the BuPTCD PVD film grows on the substrate with the (020) crystalline plane parallel to it. The latter indicates the higher RE obtained for BuPTCD in PVD film compared to PhPTCD is a consequence of its crystallinity. The broad band with maximum at 2θ around 23° is present in both diffractograms (BuPTCD and PhPTCD), being assigned to the quartz plates (substrate), as shown in Fig. 5.

3.4. Molecular Organization

Molecular organization is an important variable determining the supramolecular arrangement of the films that could impact the RE. As reported previously [32], BuPTCD molecules forming PVD film have a preferential edge-on organization: smallest axis positioned at the substrate, with the chromophore in a perpendicular position related to the substrate (Fig. 6a). Contrary, PhPTCD molecular organization in PVD film is preferentially face-on: chromophore plane parallel to the substrate (Fig. 6b) [33]. The difference in the electric dipole orientation of the perylene molecules in PVD films may influence the optical absorption process, reflecting in the RE of the films. Alessio et al. [17] reported that conductivity of perylene thin films improves with the electric field perpendicular to the chromophore, being the molecules face-to-face arranged. The same was observed by An et al. [48] for the dependence of charge transport on face-to-face molecular arranged in perylene films: higher mobility was reached when the electric field is perpendicular to the chromophore. The obtained results enforce the hypothesis that crystallinity and molecular organization of BuPTCD in PVD films are fundamental features to control the emission process (film

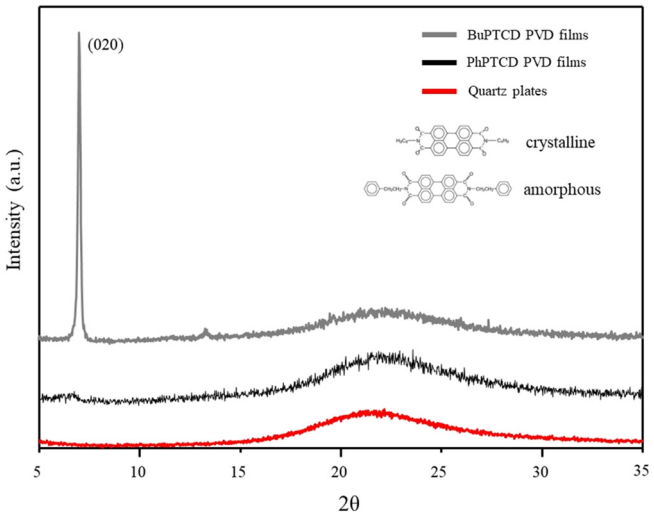

Fig. 5. X-ray diffractograms for quartz plates and of 100 nm BuPTCD and PhPTCD PVD films deposited on quartz.

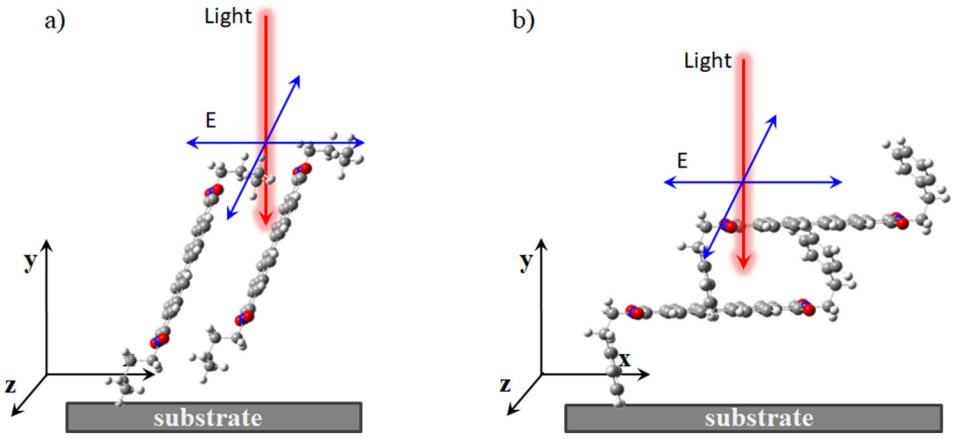

Fig. 6. Representation of the preferred molecular organization for (a) BuPTCD (edge-on: smallest axis positioned at the substrate, with the chromophore in a perpendicular position related to the substrate) and (b) PhPTCD PVD (face-on: chromophore plane parallel to the substrate) PVD films and the direction of the electric field of incident light.

RE). The latter is evident when compared with PhPTCD PVD films, which provide better RE for monomers and higher formation of J-aggregates.

4. Conclusion

The UV–Vis absorption spectra obtained for BuPTCD and PhPTCD PVD films indicate a coexistence of J- and H-aggregates in both cases, with predominance of J-aggregates, particularly to PhPTCD film. Even though J aggregates are directly related to fluorescence intensity in emission processes, the radiative efficiency (RE) of BuPTCD was 12% higher than PhPTCD in PVD films (even though RE of PhPTCD is 19% higher compared to BuPTCD when both are in solution (monomers)). Our results suggest that, besides J-aggregates (film) and RE (monomers in solution), crystallinity and molecular organization could be the reason for the higher RE found for BuPTCD PVD films: X-ray diffraction reveals an oriented crystalline phase for BuPTCD and amorphous arrangement for PhPTCD. The results are in agreement with previous FTIR work determining the face-on molecular organization of PhPTCD, and edge-on molecular organization of BuPTCD on the surface of the substrate (i.e., the parallel and perpendicular orientations of the chromophore in relation to the incoming electric field).

Acknowledgments

CAPES, CNPq, and FAPESP (processes 2013/14262-7 and 2016/09633-4) for the financial support. We are also grateful to Dr. Tibebe Lemma for the DFT calculation.

References

[1] G. Horowitz, F. Kouki, P. Spearman, D. Fichou, C. Nogues, X. Pan, F. Garnier, Evidence for n-type conduction in a perylene tetracarboxylic diimide derivative, Adv. Mater. 8 (1996) 242–245, https://doi.org/10.1002/adma.19960080312.
[2] J. Ivri, Z. Burshtein, E. Miron, R. Reisfeld, M. Eyal, The perylene derivative BASF-241 solution as a new tunable dye laser in the visible, IEEE J. Quantum Electron. 26 (1990) 1516–1520, https://doi.org/10.1109/3.102629.
[3] H. Ice, S. Icli, Ç. Sayil, Synthesis and properties of a new photostable soluble perylene dye: N,N'-di-(1-dehydroabietyl) perylene-3,4,9,10-bis(dicarboximide), Spectrosc. Lett. 31 (1998) 1643–1647, https://doi.org/10.1080/00387019808007441.
[4] X. Chu, M. Guan, Y. Zhang, Y. Li, X. Liu, Z. Zhu, B. Wang, Y. Zeng, Influences of organic–inorganic interfacial properties on the performance of a hybrid near-infrared optical upconverter, RSC Adv. 3 (2013), 23503. https://doi.org/10.1039/c3ra43143f.
[5] M.G. Ramírez, J.A. Quintana, J.M. Villalvilla, P.G. Boj, A. Retolaza, S. Merino, M.A. Díaz-García, Perylenediimide-based distributed feedback lasers with holographic relief gratings on dichromated gelatine, J. Appl. Phys. 114 (2013), 033107. https://doi.org/10.1063/1.4813873.
[6] J. Choi, W. Lee, C. Sakong, S.B. Yuk, J.S. Park, J.P. Kim, Facile synthesis and characterization of novel coronene chromophores and their application to LCD color filters, Dyes Pigments 94 (2012) 34–39, https://doi.org/10.1016/j.dyepig.2011.11.009.
[7] H. Szelke, S. Schübel, J. Harenberg, R. Krämer, A fluorescent probe for the quantification of heparin in clinical samples with minimal matrix interference, Chem. Commun. 46 (2010) 1667, https://doi.org/10.1039/b917287d.
[8] T. Ribeiro, S. Raja, A.S. Rodrigues, F. Fernandes, C. Baleizão, J.P.S. Farinha, NIR and visible perylenediimide-silica nanoparticles for laser scanning bioimaging, Dyes Pigments 110 (2014) 227–234, https://doi.org/10.1016/j.dyepig.2014.03.026.
[9] C. Keil, H. Graaf, T. Baumgärtel, I. Trenkmann, D. Schlettwein, Intralayer vs. interlayer electronic coupling in perylene imide thin films, Org. Electron. 14 (2013) 2833–2839, https://doi.org/10.1016/j.orgel.2013.07.030.
[10] E. Kozma, D. Kotowski, M. Catellani, S. Luzzati, A. Famulari, F. Bertini, Synthesis and characterization of new electron acceptor perylene diimide molecules for photovoltaic applications, Dyes Pigments 99 (2013) 329–338, https://doi.org/10.1016/j.dyepig.2013.05.011.
[11] X. Niu, W. Yang, H. Guo, J. Ren, J. Gao, Highly sensitive and selective dopamine biosensor based on 3,4,9,10-perylene tetracarboxylic acid functionalized graphene sheets/multi-wall carbon nanotubes/ionic liquid composite film modified electrode, Biosens. Bioelectron. 41 (2013) 225–231, https://doi.org/10.1016/j.bios.2012.08.025.
[12] L. Zhong, F. Xing, Y. Bai, Y. Zhao, S. Zhu, Aspartic acid functionalized water-soluble perylene diimide as "Off–On" fluorescent sensor for selective detection Cu2+ and ATP, Spectrochim. Acta A Mol. Biomol. Spectrosc. 115 (2013) 370–375, https://doi.org/10.1016/j.saa.2013.06.039.
[13] M. Ramesh, H.-C. Lin, C.-W. Chu, Organic thin film transistors as selective sensing platforms for Hg2+ ions and the amino acidcysteine, Biosens. Bioelectron. 42 (2013) 76–79, https://doi.org/10.1016/j.bios.2012.10.050.
[14] Y. Wu, B. Li, W. Wang, F. Bai, M. Liu, Coordination assisted molecular assemblies of perylene-3,4,9,10-tetracarboxylic acid with copper (II) ion at the air/water interface, Mater. Sci. Eng. C 23 (2003) 605–609, https://doi.org/10.1016/S0928-4931(03)00057-2.
[15] E. Piosik, A. Synak, T. Martyński, Influence of chlorine atoms in bay positions of perylene-tetracarboxylic acids on their spectral properties in Langmuir-Blodgett films, Spectrochim. Acta A Mol. Biomol. Spectrosc. 189 (2018) 374–380, https://doi.org/10.1016/j.saa.2017.08.043.
[16] J.Y. Kim, I.J. Chung, Photoelectrochemical processes in organic semiconductor: ambipolar perylene diimide thin film, Phys. B Condens. Matter 533 (2018) 1–4, https://doi.org/10.1016/j.physb.2017.12.063.
[17] P. Alessio, M.L. Braunger, R.F. Aroca, C. de Almeida Olivati, C.J.L. Constantino, Supramolecular organization-electrical properties relation in nanometric organic films, J. Phys. Chem. C 119 (2015) 12055–12064, https://doi.org/10.1021/acs.jpcc.5b03093.
[18] M. Ali, W.A.A. Syed, M. Zubair, N.A. Shah, A. Mehmood, Physical properties of Sb-doped CdSe thin films by thermal evaporation method, Appl. Surf. Sci. 284 (2013) 482–488, https://doi.org/10.1016/j.apsusc.2013.07.122.
[19] X. Xing, L. Zhong, L. Zhang, Z. Chen, B. Qu, E. Chen, L. Xiao, Q. Gong, Essential differences of organic films at the molecular level via vacuum deposition and solution processes for organic light-emitting diodes, J. Phys. Chem. C 117 (2013) 25405–25408, https://doi.org/10.1021/jp410547w.
[20] M. Polkehn, H. Tamura, P. Eisenbrandt, S. Haacke, S. Méry, I. Burghardt, Molecular packing determines charge separation in a liquid crystalline bisthiophene–perylene diimide donor–acceptor material, J. Phys. Chem. Lett. 7 (2016) 1327–1334, https://doi.org/10.1021/acs.jpclett.6b00277.
[21] F. Würthner, C.R. Saha-Möller, B. Fimmel, S. Ogi, P. Leowanawat, D. Schmidt, Perylene bisimide dye assemblies as archetype functional supramolecular materials, Chem. Rev. 116 (2016) 962–1052, https://doi.org/10.1021/acs.chemrev.5b00188.
[22] D. Volpati, A.E. Job, R.F. Aroca, C.J.L. Constantino, Molecular and morphological characterization of bis benzimidazo perylene films and surface-enhanced phenomena, J. Phys. Chem. B 112 (2008) 3894–3902, https://doi.org/10.1021/jp077588h.

[23] P.A. Antunes, C.J.L. Constantino, R. Aroca, J. Duff, Reflection absorption infrared spectra of thin solid films. Molecular orientation and film structure, Appl. Spectrosc. 55 (2001) 1341–1346, https://doi.org/10.1366/0003702011953450.
[24] J.M. Hsu, L. Rieth, S. Kammer, M. Orthner, F. Solzbacher, Effect of thermal and deposition processes on surface morphology, crystallinity, and adhesion of Parylene-C, Sens. Mater. 20 (2008) 87–102.
[25] S.-G. Liu, G. Sui, R.A. Cormier, R.M. Leblanc, B.A. Gregg, Self-organizing liquid crystal perylene diimide thin films: spectroscopy, crystallinity, and molecular orientation, J. Phys. Chem. B 106 (2002) 1307–1315, https://doi.org/10.1021/jp013254v.
[26] F. Würthner, Perylene bisimide dyes as versatile building blocks for functional supramolecular architectures, Chem. Commun. (2004) 1564–1579, https://doi.org/10.1039/B401630K.
[27] D. Liu, S. De Feyter, M. Cotlet, U.-M. Wiesler, T. Weil, A. Herrmann, K. Müllen, F.C. De Schryver, Fluorescent self-assembled polyphenylene dendrimer nanofibers, Macromolecules 36 (2003) 8489–8498, https://doi.org/10.1021/ma0348573.
[28] P. Yan, A. Chowdhury, M.W. Holman, D.M. Adams, Self-organized perylene diimide nanofibers, J. Phys. Chem. B 109 (2005) 724–730, https://doi.org/10.1021/jp046133e.
[29] Z. Chen, V. Stepanenko, V. Dehm, P. Prins, L.D.A. Siebbeles, J. Seibt, P. Marquetand, V. Engel, F. Würthner, Photoluminescence and conductivity of self-assembled π–π stacks of perylene bisimide dyes, Chem. Eur. J. 13 (2007) 436–449, https://doi.org/10.1002/chem.200600889.
[30] T.E. Kaiser, H. Wang, V. Stepanenko, F. Würthner, Supramolecular construction of fluorescent J-aggregates based on hydrogen-bonded perylene dyes, Angew. Chem. Int. Ed. 46 (2007) 5541–5544, https://doi.org/10.1002/anie.200701139.
[31] T.E. Kaiser, V. Stepanenko, F. Würthner, Fluorescent J-aggregates of core-substituted perylene bisimides: studies on structure–property relationship, nucleation–elongation mechanism, and sergeants-and-soldiers principle, J. Am. Chem. Soc. 131 (2009) 6719–6732, https://doi.org/10.1021/ja900684h.
[32] J.D. Fernandes, P.H.B. Aoki, R.F. Aroca, W.D. Macedo Junior, A.E. de Souza, S.R. Teixeira, M.L. Braunger, C. de A. Olivati, C.J.L. Constantino, Supramolecular architecture and electrical properties of a perylene derivative in physical vapor deposited films, Mater. Res. 18 (2015) 127–137, https://doi.org/10.1590/1516-1439.349614.
[33] J.D. Fernandes, P. Alessio, M.R.M. Silva, R.F. Aroca, A.E. de Souza, C.J.L. Constantino, Physical vapor deposited films of a perylene derivative: supramolecular arrangement and thermal stability, Mater. Res. 20 (2017) 882–890, https://doi.org/10.1590/1980-5373-mr-2016-0692.
[34] R. Mercadante, M. Trsic, J. Duff, R. Aroca, Molecular orbital calculations of perylenetetracarboxylic monoimide and bisimide. Alkyl derivatives and heteroatom analogs, J. Mol. Struct. THEOCHEM 394 (1997) 215–226, https://doi.org/10.1016/S0166-1280(96)04837-3.
[35] R.F. Aroca, C.J.L. Constantino, Surface-enhanced Raman scattering: imaging and mapping of Langmuir—Blodgett monolayers physically adsorbed onto silver island films, Langmuir 16 (2000) 5425–5429, https://doi.org/10.1021/la991478n.
[36] K.D. Belfield, M.V. Bondar, O.V. Przhonska, K.J. Schafer, Photophysical characterization of 2,9-bis(7-benzothiazole-9,9′-didecylfluoren-2-yl)perylene diimide: a new standard for steady-state fluorescence anisotropy, J. Photochem. Photobiol. A Chem. 151 (2002) 7–11, https://doi.org/10.1016/S1010-6030(02)00176-4.
[37] M. Adachi, Y. Murata, S. Nakamura, Spectral similarity and difference of naphthalenetetracarboxylic dianhydride, perylenetetracarboxylic dianhydride, and their derivatives, J. Phys. Chem. 99 (1995) 14240–14246, https://doi.org/10.1021/j100039a009.
[38] A. Kam, R. Aroca, J. Duff, C.P. Tripp, Evolution of the molecular organization in bis(n-propylimido)perylene films under thermal annealing, Chem. Mater. 10 (1998) 172–176, https://doi.org/10.1021/cm970299t.
[39] L.B.-Å. Johansson, H. Langhals, Spectroscopic studies of fluorescent perylene dyes, Spectrochim. Acta A: Mol. Spectrosc. 47 (1991) 857–861, https://doi.org/10.1016/0584-8539(91)80272-K.
[40] R.M. Hochstrasser, M. Kasha, Application of the exciton model to mono-molecular lamellar systems, Photochem. Photobiol. 3 (1964) 317–331, https://doi.org/10.1111/j.1751-1097.1964.tb08155.x.
[41] M. Kasha, H.R. Rawls, M. Ashraf El-Bayoumi, The exciton model in molecular spectroscopy, Pure Appl. Chem. 11 (1965)https://doi.org/10.1351/pac196511030371.
[42] K.Y. Burshtein, A.A. Bagatur'yants, M.V. Alfimov, MO calculations on the absorption spectra of organic dimers. The interaction energy between dipole moments of electronic transitions in monomers and the shape of absorption bands, Chem. Phys. Lett. 239 (1995) 195–200, https://doi.org/10.1016/0009-2614(95)00443-8.
[43] C.J.L. Constantino, T. Lemma, P.A. Antunes, R. Aroca, Single molecular detection of a perylene dye dispersed in a Langmuir-Blodgett fatty acid monolayer using surface-enhanced resonance Raman scattering, Spectrochim. Acta A Mol. Biomol. Spectrosc. 58 (2002) 403–409.
[44] L. Zou, A. You, J. Song, X. Li, M. Bouvet, W. Sui, Y. Chen, Cation-induced self-assembly of an amphiphilic perylene diimide derivative in solution and Langmuir–Blodgett films, Colloids Surf. A Physicochem. Eng. Asp. 465 (2015) 39–46, https://doi.org/10.1016/j.colsurfa.2014.10.021.
[45] Y. Dong, J.W.Y. Lam, A. Qin, J. Sun, J. Liu, Z. Li, J. Sun, H.H.Y. Sung, I.D. Williams, H.S. Kwok, B.Z. Tang, Aggregation-induced and crystallization-enhanced emissions of 1,2-diphenyl-3,4-bis(diphenylmethylene)-1-cyclobutene, Chem. Commun. (2007) 3255, https://doi.org/10.1039/b704794k.
[46] Z. Li, Y. Dong, B. Mi, Y. Tang, M. Häussler, H. Tong, Y. Dong, J.W.Y. Lam, Y. Ren, H.H.Y. Sung, K.S. Wong, P. Gao, I.D. Williams, H.S. Kwok, B.Z. Tang, Structural control of the photoluminescence of silole regioisomers and their utility as sensitive regiodiscriminating chemosensors and efficient electroluminescent materials, J. Phys. Chem. B 109 (2005) 10061–10066, https://doi.org/10.1021/jp0503462.
[47] T.-S. Hsiao, S.-L. Deng, K.-Y. Shih, J.-L. Hong, Crystallization-enhanced emission through hydrogen-bond interactions in blends containing hydroxyl-functionalized azine and poly(4-vinyl pyridine), J. Mater. Chem. C 2 (2014) 4828–4834, https://doi.org/10.1039/C4TC00005F.
[48] N. An, Y. Shi, J. Feng, D. Li, J. Gao, Y. Chen, X. Li, N-channel organic thin-film transistors based on a soluble cyclized perylene tetracarboxylic diimide dimer, Org. Electron. 14 (2013) 1197–1203, https://doi.org/10.1016/j.orgel.2013.02.012.